Journal of Thermal Analysis, Vol. 48 (1997) 247-258

FERRIMAGNETIC SPINELS IN HYDROTHERMAL AND THERMAL TREATMENT OF $Mn_xFe_{2-2x}(OH)_{6-4x}$

W. Wolski, E. Wolska, J. Kaczmarek and P. Piszora

Department of Magnetochemistry, Adam Mickiewicz University, Grunwaldzka 6, PL-60780 Poznań, Poland

(Received September 10, 1995; in revised form July 2, 1996)

Abstract

Products of hydrothermal treatment of the initial amorphous system $Mn_xFe_{2-2x}(OH)_{6-4x}$ for $0 \leq x \leq 1$ in 0.1 x intervals, and products of their further thermal treatment, were examined by chemical analysis, X-ray, IR, and DTA techniques supported by magnetic measurements. After hydrothermal growth for low x, hematite and goethite phases occurred. Although the goethite phase was still identifiable at $x=0.6$, formation of a solid solution with the isostructural groutite was not found. The ferrimagnetic spinel phase, which resists heating up to 400°C, was present at $0.5 \leq x \leq 0.9$. At higher temperatures, it transformed into the rhombohedral hematite type phase or into the cubic bixbyite phase. At $T \geq 900$°C, a ferrimagnetic spinel structure reappeared up to $x=0.8$. For $x=0.9$, the low- and high-temperature forms of the hausmannite phase occurred, for $x=1$ passing from one form into another through Mn_5O_8 and partritgeite.

For a primary mixture $Mn_{0.5}Fe(OH)_4$, corresponding to the manganese ferrite structure, the lattice parameter of which passes from 8.43 Å through 8.33 Å to 8.50 Å, the probable crystallochemical formula was suggested.

Keywords: ferrimagnetic spinels, system $Mn_xFe_{2-2x}(OH)_{6-4x}$

Introduction

Coprecipitated mixtures of Mn(II)/Fe(III) hydroxides, sometimes accompanied by other divalent cations, are precursors of products with numerous technical applications. This is a factor contributing to why these systems are studied so extensively [1–7]. Though they may play only a role of molecularly mixed component for the production of fired ferrites, the main emphasis is now laid on their direct transformation into ferrimagnetic phases by simple maturation, ageing, storage, hydrothermal growth of whatever we call the process involved. These very easily formed spinel type phases have complicated, not clear-cut chemical formulae, not to mention the crystallochemical ones, the basic tool necessary to find the relation between the magnetic properties and structure. The problem is created not only by the equilibrium $Mn^{2+}+Fe^{3+} \rightleftarrows Mn^{3+}+Fe^{2+}$ [8], but also by the fact that manganese has a tendency to form enormous numbers of individuals with various valencies and dif-

0368–4466/97/ $ 5.00

John Wiley & Sons, Limited
Chichester

ferent O/Mn ratios [9, 10], with the vacancies spread over different positions of the sublattices [11–13].

For certain x values, the initially amorphous mixtures $Mn_xFe_{2-2x}(OH)_{6-4x}$ are converted into ferrimagnetic species when stored as water suspensions well below 100°C, and the higher the temperature, the shorter the time of transformation [14]. Details of the ageing of amorphous systems $Mn_xFe_{2-2x}(OH)_{6-4x}$ at 100°C within the range $0 \leq x \leq 1$, and the consequences of higher temperatures on the hydrothermally obtained products, are presented below.

Experimental

Aqueous solutions of titrated 0.25 *M* Mn(II) and 0.25 *M* Fe(III) nitrates, mixed together in the desired proportions to give the hydroxide mixtures $Mn_xFe_{2-2x}(OH)_{6-4x}$ in $0.1x$ intervals, were treated by constant stirring with 2 *M* NaOH till *pH* 9.5 was reached, to ensure full Mn(II) precipitation and at the same time to avoid oxidation to Mn_3O_4 and β-MgOOH at higher *pH*. The washed and filtered hydroxides were placed in teflon vessels and were stored in the form of water suspensions in autoclaves at 100°C for 24 h. The products were spread thinly on glass plates and dried for 48 h at 30°C. Chemical analysis, supported by atomic absorption spectrometry, revealed negligible deviations from the nominal Mn/Fe ratios.

X-ray powder diffraction analysis was performed with a TUR-61 diffractometer equipped with an HZG-3 proportional counter spectrometer joined with counting components and a computerized impulse printing unit, using FeK_α radiation. Differential thermal analysis was carried out on a Hungarian Q1000 MOM model, and infrared absorption spectra were recorded on a Perkin-Elmer 180 spectrophotometer, using CsI pellets. Saturation magnetization was measured on a magnetic balance designed in our laboratory, and thermomagnetograms were recorded on a GEAR X-Y Recorder 240. The X-ray quantitative analysis of the individual components formed by hydrothermal and thermal treatment was performed by mixing mechanically in a mortar different quantities of the corresponding crystalline standard preparations, suspending them in a non-polar liquid (CCl_4) and shaking in a vibrator to assure the best homogeneity. After evaporation of the liquid and drying of the mixtures at 30°C, the changes in the integral intensities of the most sensitive X-ray reflections were utilized to draw the curves, from which the content of the examined phase in the studied preparations was then evaluated.

Results and discussion

Extremely many factors determine the formation of given compositions from the same components $M(OH)_2/Fe(OH)_3$. In the case of the $Mn(OH)_2/Fe(OH)_3$ system, the freshly formed amorphous 'molecular' mixtures undergo transformation under the hydrothermal conditions described above into the products presented in Fig. 1. It can be seen that pure $Fe(OH)_3$ is converted into hematite and goethite, the hematite phase being visible up to $x=0.4$, and the goethite phase up to $x=0.6$, as dem-

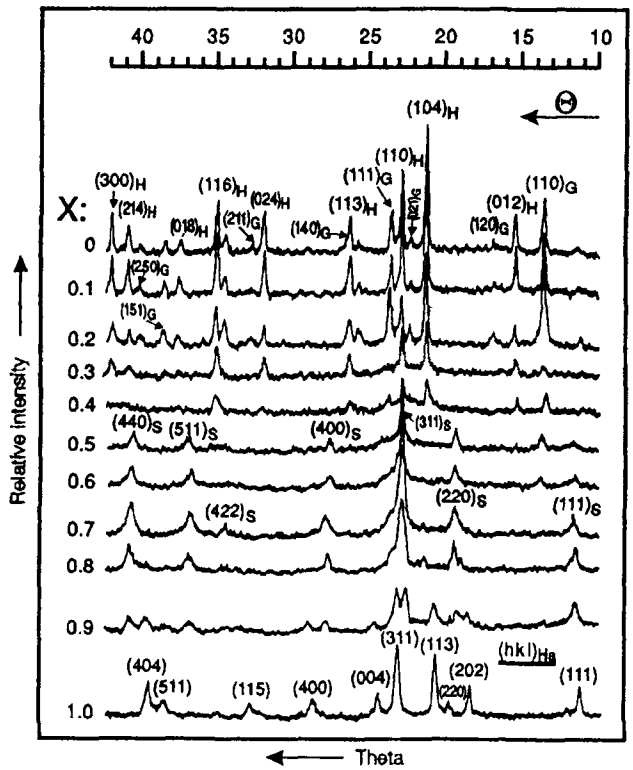

Fig. 1 X-ray diffractograms of hydrothermal products of $Mn_xFe_{2-2x}(OH)_{6-4x}$. H – hematite, G – goethite, S – spinel, Ha – hausmannite

onstrated by its most characteristic (110) reflection. The question might arise as to whether the goethite phase is pure or is a solid solution with the isomorphous groutite, α-MnOOH. Such a solid solution has not been found in nature yet and its synthesis has only a short history. The references indicate four positions [15–18]. According to [15], goethite incorporates ca. 15 mol% Mn isostructurally. In [16], 8 mol% is suggested. Cornell and Giovanoli [17] confirm the results in [15], while [18] gives the limit of isomorphous incorporation of Mn at 34 mol%. In each case the preparatory conditions were different, and they differ from those in our procedure too. Though the unit cell parameters of pure goethite are very well known and those of groutite have also been satisfactorily determined [19–21], it is striking that to date the most convincing argument is still missing, i.e. how the experimental points obtained satisfy Vegard's law. In the case presented here, we did not observe the formation of α-(Fe,Mn)OOH, though the experimental conditions supplied enough oxygen to oxidize Mn^{2+} to Mn^{3+}. For $0.5 \leq x \leq 0.9$, the main peaks of the spinel phase appear, and are best developed at $x=0.7$. As will be seen below, magnetic measurements prove that the formation of this ferrimagnetic spinel structure occurs even at $x=0.3$. The X-ray patterns of the preparation with $x=0.9$ demon-

strates partial tetragonal distortion of the spinel structure, indicative of hausmannite, the only manganese phase identified for $x=1$.

Just as the X-ray patterns did not reveal any distinctly marked shifts in θ with increasing x for the goethite phase, in the IR spectra (Fig. 2) the positions of the most characteristic OH bands of α-FeOOH, i.e. those at ~795 cm^{-1} and ~895 cm^{-1} in the bending vibration region, show no sign of displacement with changing x. The last band is still visible at $x=0.6$, confirming the limit of the presence of α-FeOOH found by X-ray analysis. The hematite and goethite Me–O stretching vibration bands in section C of Fig. 2 partially overlap and give rather a corrugated line at 400–650 cm^{-1}; at 0.3–0.4x, this changes into two hollows, the second one at 550 cm^{-1} displacing its position stepwise to 580 cm^{-1} as a result of the deteriorating hematite structure and crumbling goethite crystallites. No absorptions are observed which relate to the increasing presence of the ferrimagnetic spinel phase for $x=0.6$ and 0.7; we are inclined to interpret this in terms of its very small crystallite dimensions, which, according to Scherrer's equation, do not exceed 180 Å. From $x=0.7$ up to 0.9, a broad hollow centred at ~900 cm^{-1} deepens more and more. We presume that this is caused by partial transformation of the original manganese hydroxide into nearly amorphous feitknechtite, β-MnOOH,

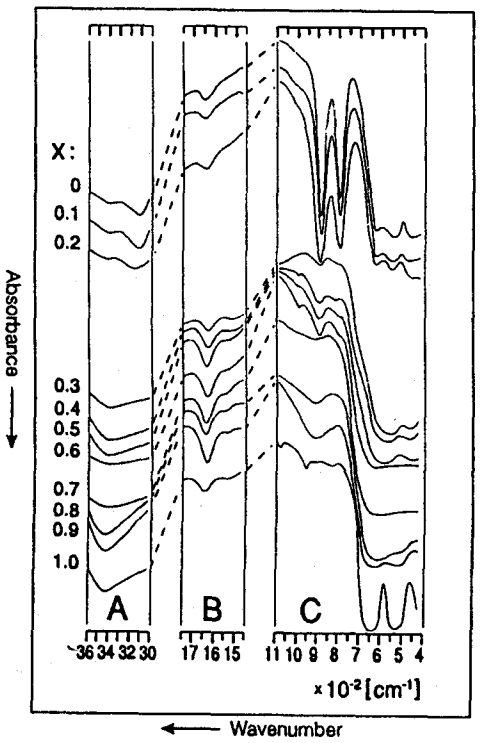

Fig. 2 IR spectra after hydrothermal storage of $Mn_xFe_{2-2x}(OH)_{6-4x}$

which would explain the deep bands in sections A and B. At $x=1$, the crystallites grew sufficiently to allow observation of the three small separate bands at ~815, ~950 and ~1070 cm^{-1} for this phase [22], which remained unidentifiable with the X-ray technique. Three bands at lower frequencies for $x=1$ belong to the hausmannite structure.

The changes in the hydrothermally obtained products when they are heated at 10°C min^{-1} are demonstrated by the DTA curves in Fig. 3. We see that the preparations do not distinctly display weakly bound water for all x. If present, it is easily evolved at about 125°C or below. The preparations richest in this unconstitutional water are those originating from $x=0.3$ and 0.4. On heating for 5 h at 150°C, they lose 8 and 9.5% H_2O respectively, while the others, with the exception of the sample from $x=0.5$ (~4% H_2O), lose only ~1% H_2O at that temperature. The endothermic effects at ~330°C (for $0 \leq x \leq 0.4$) are those of goethite phase destruction, while those at ~260°C down to $x=0.9$ presumably stem from traces of unconverted initially amorphous material and the quasi-amorphous state of the assumed β-MnOOH at higher x values. The exothermic effects at ~530°C ($x=0.3$, 0.4) relate to decomposition of the spinel phase into the rhombohedral α-$(Fe,Mn)_2O_3$. This decomposition, connected with the oxidation of Mn^{2+}, is more acute at $x=0.5$ and $x=0.6$, when the spinel phase predominates after hydrothermal growth. The second

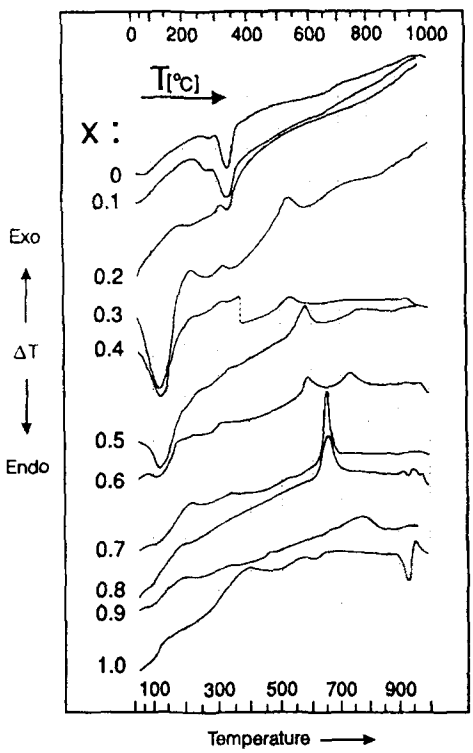

Fig. 3 DTA curves of samples after hydrothermal growth of $Mn_xFe_{2-2x}(OH)_{6-4x}$

exothermic effect, near 750°C, is due to the formation of cubic bixbyite, $(Mn,Fe)_2O_3$. These reactions, the oxidation and transformation into bixbyite, occur simultaneously at $x=0.7$ and 0.8, giving an acute exothermic effect at ~650°C. At $x=0.9$, the same transformations take place at ~780°C. The exothermic effect at 400°C for $x=1$ is connected with the formation of a species $Mn_2^{II}\,Mn_3^{IV}\,O_8$, while the small endothermic peak at ~600°C corresponds to the endothermic transition $Mn_5O_8 \rightarrow \alpha\text{-}Mn_2O_3$ (partritgeite). The deep peak at ~960°C is an indication of the conversion of partritgeite into hausmannite [23, 24] and not to the transition $\alpha \rightarrow \beta$-hausmannite [25], since, as a rule, polymorphous transitions do not produce deep, acutely marked effects in DTA.

In order to say something more about the spinel phase formed after hydrothermal treatment, at $0.5 \leq x \leq 0.9$, we first tried to establish its thermal resistance. As X-ray charts for $x=0.5$, i.e. for the composition corresponding to 'pure' manganese ferrite, $MnFe_2O_4$, recorded as the sample was subjected progressively to increasing temperatures, for 5 h each, are presented in Fig. 4. The spinel phase first formed hydrothermally can resist such a heating procedure up to 400°C. Between 450 and 500°C, the sample is transformed into a phase with the hematite structure, well crystallized at 500°C. However, as a unique rhombohedral phase of the manganese-containing hematite, it exists only up to 600°C. At higher temperatures, at its expense (compare, for example, the intensity changes in the $(300)_H$- and $(214)_H$ lines) a cubic structure of the bixbyite phase appears beside it. As individual components, they coexist up to 900°C. The bixbyite phase then transforms into the real manganese ferrite, at 1000°C, partly extending the amount of the hematite phase as well. It is necessary for the temperature to be raised up to 1150°C, in order to get the one-phase pattern of pure manganese ferrite, $MnFe_2O_4$.

The quantitative relationships between the existing crystalline phase for the whole range of x studied by X-ray analysis are shown in Fig. 5. The species assigned in Fig. 5 as 'spinel structure' changes its lattice parameter, a_0, for $x=0.5$ horizontally from 8.43 Å (100°C) to 8.33 Å (400°C). However, the last sample in the row for $x=0.5$ has $a_0=8.50$ Å, and the appropriate stoichiometry for sintered $MnFe_2O_4$. Vertically downwards in the first column, a_0 does not change appreciably. For $x=1$, the low and high-temperature forms of tetragonal hausmannite give $a_0=8.15$ Å and $c_0=9.46$ Å. On conversion from one type into the other, it passes through partial formation of the Mn_5O_8 phase, transforming further into $\alpha\text{-}Mn_2O_3$. Nearly pure Mn_3O_4 is formed at 800°C, while at higher temperatures the amount of $\alpha\text{-}Mn_2O_3$ again rises slightly. Such a reversibility was observed recently [24]. Thorough investigations of the intensities of the X-ray reflections and of the IR spectra of the products of thermal treatment at higher temperatures allowed us, at least in the case $x=0$, to prove that the hematite phase is in fact that of hydrohematite [26–28]. During heating at as low as 200°C, the 13% of goethite for $x=0.5$ disappears, not undergoing conversion into the crystalline hematite phase, and the process does not improve the magnetization. The same holds for $x=0.6$.

The magnetic properties of samples obtained by hydrothermal storage of the amorphous system $Mn_xFe_{2-2x}(OH)_{6-4x}$ at 100°C, and their changes when the sam-

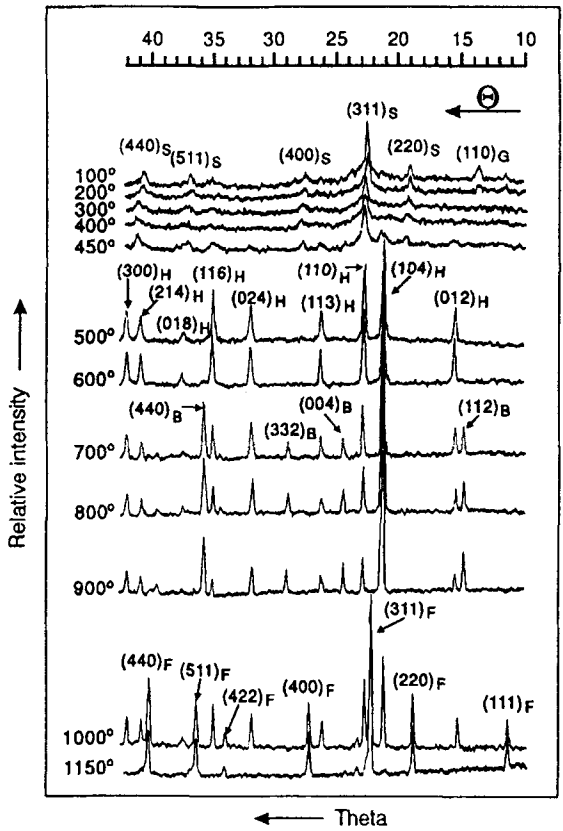

Fig. 4 X-ray patterns of hydrothermal product of $Mn_{0.5}Fe(OH)_4$ heated at various temperatures. B – bixbyite, F – manganese ferrite

ples are heated at different temperatures in air, are illustrated in Fig. 6. It may be seen that the ferrimagnetic spinel phase indeed starts to appear as early as $x=0.3$. The highest saturation magnetization is displayed by the sample from the primary hydroxide composition $Mn_{0.7}Fe_{0.6}(OH)_{3.2}$, and not from the $Mn_{0.5}Fe(OH)_4$, necessary to obtain stoichiometric $MnFe_2O_4$. However, during thermal treatment, as the temperature rises and the ferrimagnetism reappears after transition through non-magnetic stages, the maximum in σ is gradually displaced towards that for the real $MnO{\cdot}Fe_2O_3$ stoichiometry, until the finally attainment of the $\sigma_{20°C}$ value known for $MnFe_2O_4$ obtained by the sintering procedure [29].

The Curie points of the magnetic products formed during hydrothermal storage are situated in the interval 330–375°C. To illustrate these characteristics, we have chosen two cases: the product from ageing of the composition $Mn_{0.5}Fe(OH)_4$ (Fig. 7.1), i.e. a precursor of sintered ferrite with stoichiometry $MnFe_2O_4$, and that from $Mn_{0.7}Fe_{0.6}(OH)_{3.2}$, exhibiting the maximum specific saturation magnetization $\sigma_{20°C}$ after hydrothermal treatment. The Curie point, T_c, of the sample from

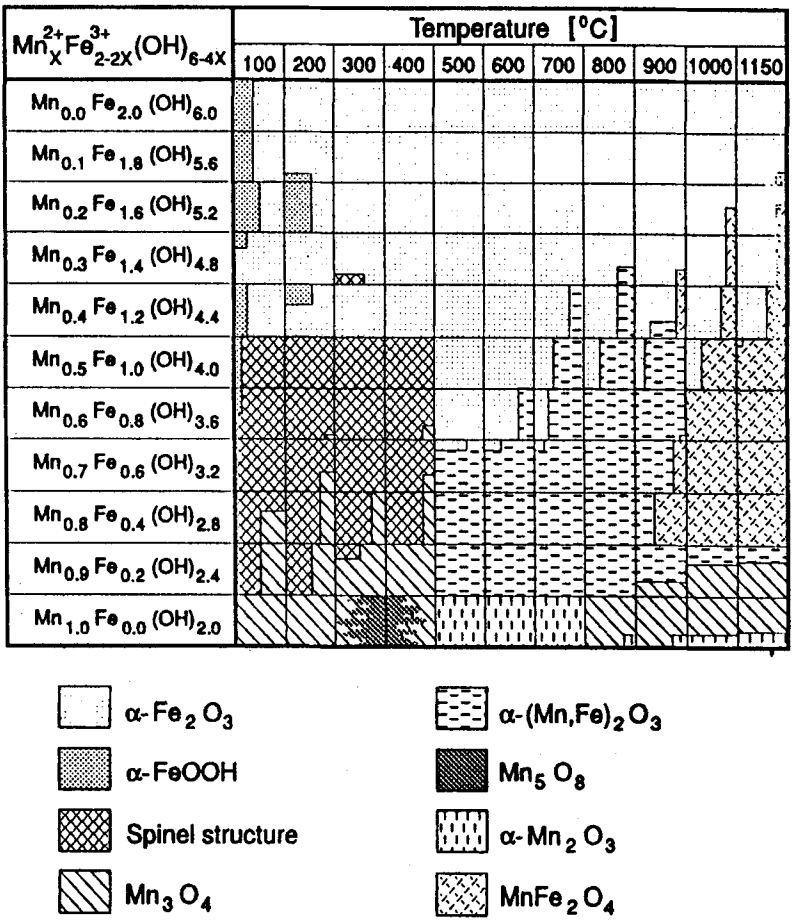

Fig. 5 Quantitative participation of crystalline phases formed during heating of hydrothermally obtained products, based on X-ray analysis

$Mn_{0.5}Fe(OH)_4$, is much higher (~375°C) than expected for $MnFe_2O_4$ (300°C [29]). During cooling of the sample, it does not lose magnetization, as a result of the starting transformation of manganese ferrite into non-magnetic manganese and iron sesquioxides at 300°C [30]; it rather gains in magnetization. The process is overcompensated by the loss of unbound H_2O and of OH groups from α-FeOOH. The slight bulge in the primary curve 1 within the region 220–350°C is a sign of the conversion into another ferrimagnetic spinel phase as the temperature rises during T_c recording. The T_c at ~335°C (curve 2) was comparable to the T_c of sintered $MnFe_2O_4$ quenched from 1150°C [31].

A multitude of proposals have been made concerning the crystallochemical formula of a simple, stoichiometric manganese ferrite sintered at high temperature, in an attempt to attain agreement between the theoretical magnetic moment of 5 μ_B

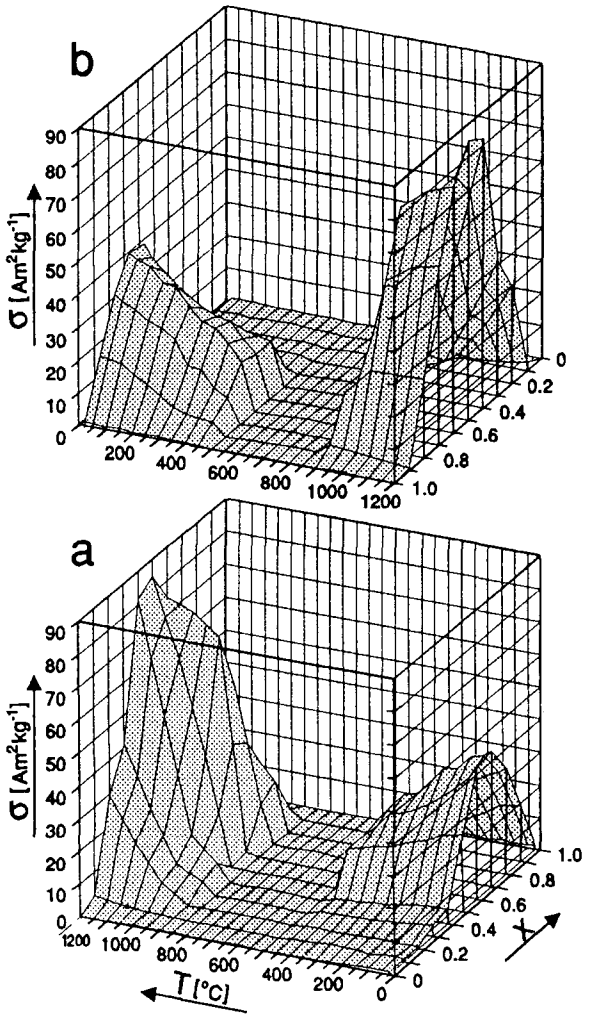

Fig. 6 Room-temperature specific saturation magnetization, $\sigma_{20°C}$, as a function of composition and thermal treatment of hydrothermally obtained products from $Mn_xFe_{2-2x}(OH)_{6-4x}$. b: 'a' revolved by 180°

and the observed 4.6 μ_B. It is far more complicate to find the corresponding cation distribution when 'manganese ferrite' is formed by a wet method. It is enough in this respect to compare the final results concerning samples of manganese ferrite from the same wet method, studied by very sophisticated instrumental techniques in [32] and [33]. However, there are some slight hints indicating at least what kind of ferrimagnetic species with spinel structure are formed under the conditions described here. Exemplifying the case on the primary composition $Mn_{0.5}Fe(OH)_4$, for the future pure $MnFe_2O_4$, let us set forth the following circumstances: $Mn_{0.5}Fe(OH)_4$,

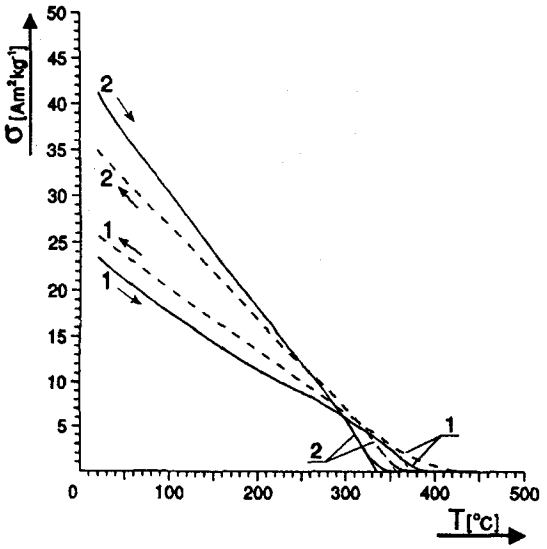

Fig. 7 Thermomagnetograms of hydrothermally obtained products from originally amorphous $Mn_xFe_{2-2x}(OH)_{6-4x}$. 1) $x=0.5$; 2) $x=0.7$

with the proper $MnFe_2O_4$ stoichiometry, $MnO{\cdot}Fe_2O_3$, because of iron engaged in 13% of α-FeOOH, causes an excess of Mn ($1.0695MnO{\cdot}1.0Fe_2O_3$) in the spinel phase and the system may be regarded as a solid solution of $Mn_3O_4/MnFe_2O_4$. The spinel phase after hydrothermal growth has a lattice parameter of 8.43 Å, while the ferrimagnetic spinel phase formed from this after sintering at 1150°C has $a_0=$ 8.50 Å. Before this, successive heating at 200, 300 and 400°C causes a decrease in a_0 to the limit 8.33 Å. This is the parameter of ferrimagnetic maghemite, γ-Fe_2O_3, with a defective spinel structure: $Fe[Fe_{5/3}\square_{1/3}]O_4$. Divalent manganese undergoes oxidation to higher valencies in the solid state, causing the occurence of vacancies: $3Mn^{2+}\rightarrow 2Mn^{3+}+\square$. On the other hand, trivalent manganese ions display a strong affinity for the octahedral sites of the spinel lattice [34], and in the octahedral sites high-spin coordination Fe^{3+} and Mn^{3+} have exactly the same radii: 0.645 Å [35]. Further, it has been proved that the diffusion of cations between sublattices A and B in manganese ferrite starts at as low as 250°C [33]. Iodimetric titration and EDTA back-titration with Zn^{2+} solution revealed that, after the hydrothermal operation, about 33% of the Mn^{2+} from the initial 0.5MnO has been oxidized, whereas in the spinel phase with $a_0=8.33$ Å after final heating at 400°C, the reaction for divalent manganese was negative. The magnetization curves run towards zero during the T_c recording (Fig. 7), but before reaching it they display slight humps, beginning at about 220°C. In Fig. 6, the slopes in the decreasing magnetization as the samples are heated to higher and higher temperatures do show some restraints, beginning from ~250°C (see the curve in Fig. 6a for $x=0.5$), before they fall rapidly to zero at ~500°C. These two effects together prove that the preliminary ferrimagnetic

phase undergoes transformations leading to ferrimagnetic species with higher T_c and smaller a_o before it becomes a simple, sintered, stoichiometric manganese ferrite. These arguments allow use of the relationship between the lattice parameter and the amount of cation vacancies when all the vacancies occur at the same sites, here in sublattice B, i.e. between the a_o for $MnFe_2O_4$ free of vacancies and a_o for γ-$(Mn,Fe)_2O_3$ with 0.33 vacancies. If it is assumed that all the vacancies in the sample after hydrothermal treatment are caused by the oxidized manganese, the quantitative cation distribution may be given as $Mn^{2+}_{0.601}Fe^{3+}_{0.399}[Fe^{3+}_{1.567}Mn^{3+}_{0.300}\ \square_{0.133}]O_4$ and after further heating up to 400°C and the attainment of a_o=8.33 Å, the formula may be written as $Fe^{3+}[Fe^{3+}_{0.833}Mn^{3+}_{0.833}\ \square_{0.333}]O_4$ or γ-$(Fe^{3+}_{1.375}\ \square_{0.625})O_3$.

Conclusions

The formation of ferrimagnetic spinels from amorphous mixtures of $Mn(OH)_2/Fe(OH)_3$ subjected to hydrothermal crystallization under the conditions applied was possible for $0.5 \leq x \leq 0.9$, although a single phase was formed only for $x=0.7$. However, magnetic measurements, the most sensitive method, proved their presence within the range $0.3 \leq x \leq 0.9$. On thermal treatment after hydrothermal maturation, the system $Mn^{2+}_xFe^{3+}_{2-2x}(OH)_{6-4x}$ passes through various crystalline states before the formation of manganese ferrite, $MnFe_2O_4$, or its solid solutions with stoichiometries different from Mn:Fe=1:2, at 1150°C.

On the example of $Mn_{0.5}Fe_{1.0}(OH)_4$, the precursor of manganese ferrite, thorough chemical analysis, measurements of the unit cell parameter and examination of the magnetic behaviour suggested the probable stages of conversion up to the product, $MnFe_2O_4$.

The higher Curie point (~375°C) of the species prepared thermally from $Mn_{0.5}Fe_{1.0}(OH)_4$ is connected with its smaller unit cell parameter (8.43 Å) in comparison with that of a real $MnFe_2O_4$ ferrite (a=8.50 Å; T_c=300°C), since the Curie temperatures increase as the distances between the paramagnetic ions decrease, which is the case in a smaller unit cell.

* * *

We are grateful to KBN (The State Committee for Scientific Research, Poland) for grant No. 3 T09A 064 08, which contributed substantially to the materialization of this project.

References

1 M. T. Johnson, A. Noordermeer, M. M. E. Severin and W. A. M. Meeuwissen, J. Magn. Magn. Mater., 116 (1992) 169.
2 E. Blums, M. M. Maiorov and G. Kronkalns, IEEE Trans. Magn., 29 (1993) 3267.
3 G. M. Sutariya, R. V. Upadhyay and R. V. Mehta, J. Colloid Interface Sci., 155 (1993) 152.
4 E. Segal, M. Brezeanu, V. Bujoreanu and C. Gheorghies, Thermochim. Acta, 196 (1992) 7.
5 R. V. Upadhyay, K. J. Davies, S. Wells and S. W. Charles, J. Magn. Magn. Mater., 132 (1994) 249; 139 (1994) 249.
6 R. V. Mehta, R. V. Upadhyay, B. A. Dasannacharya, P. S. Goyal and K. S. Rao, J. Magn. Magn. Mater., 132 (1994) 153.

7 Y. Yamamoto and A. Makino, J. Magn. Magn. Mater., 133 (1994) 500.
8 F. K. Lotgering, J. Phys. Chem. Solids, 25 (1964) 95.
9 O. Glemser, G. Gattow and H. Meisiek, Z. Anorg. Allg. Chem., 309 (1961) 1.
10 H. R. Oswald and M. J. Wampetich, Helv. Chim. Acta, 50 (1967) 2023.
11 J. Kaczmarek and E. Wolska, J. Solid State Chem., 103 (1993) 387.
12 J. Kaczmarek and E. Wolska, Solid State Ionics, 63–65 (1993) 633.
13 E. Wolska and J. Kaczmarek, Solid State Phenomena, 39–40 (1994) 153.
14 W. Wolski and J. Kaczmarek, J. Magn. Magn. Mater., 40 (1983) 190.
15 W. Stiers and U. Schwertmann, Geochim. Cosmochim. Acta, 49 (1985) 1909.
16 R. E. Vandenberghe, A. E. Verbeeck, E. De Grave and W. Stiers, Hyperfine Interact., 29 (1986) 1157.
17 R. M. Cornell and R. Giovanoli, Clays Clay Miner., 35 (1987) 11.
18 M. H. Ebinger and D. G. Schulze, Clays Clay Miner., 37 (1989) 151.
19 J. W. Gruner, Am. Miner., 32 (1947) 654.
20 R. L. Collin and W. N. Lipscomb, Acta Crystallogr., 2 (1949) 104.
21 L. S. D. Glasser and L. Ingram, Acta Crystallogr., B 24 (1968) 1233.
22 J. Kaczmarek, PhD Thesis, Poznań 1990.
23 J. Pattanayak and V. S. Rao, J. Mater. Sci. Lett., 8 (1989) 1405.
24 J. Pattanayak and H. S. Maiti, J. Mater. Sci. Lett., 9 (1990) 414.
25 H. J. Van Hook and M. L. Keith, Am. Miner., 43 (1958) 69.
26 E. Wolska, Z. Kristallogr., 154 (1981) 69.
27 E. Wolska, Solid State Ionics, 28–30 (1988) 1349.
28 E. Wolska and U. Schwertmann, Z. Kristallogr., 189 (1989) 223.
29 J. Smit and H. P. J. Wijn, Ferrites, Philips, Eidhoven 1959, p. 157.
30 H. H. Kedesdy and A. Tauber, J. Am. Ceram. Soc., 39 (1956) 425.
31 F. K. Lotgering, Philips Res. Repts, 20 (1965) 320.
32 M. A. Denecke, W. Gunßer, G. Buxbaum and P. Kuske, Mater. Res. Bull., 27 (1992) 507.
33 H. Yasuoka, A. Hirai, T. Shinio, M. Kiyama, Y. Bando and T. Tokada, J. Phys. Soc. Jap., 22 (1967) 174.
34 J. B. Goodenough and A. L. Loeb, Phys. Rev., 98 (1955) 391.
35 R. D. Shannon, Acta Crystallogr., A 32 (1976) 751.